CLM-P857

CLM-P857

Resistive ballooning modes in the second stable regime

T.C. Hender
K. Grassie
H.P. Zehrfeld

UK ATOMIC ENERGY AUTHORITY

Culham Laboratory

CLM-P857

Resistive ballooning modes in the second stable regime

T.C.Hender,
UKAEA–Euratom Fusion Association
Culham Laboratory, Abingdon, Oxon, OX143DB, UK.

K.Grassie, H.P.Zehrfeld
Max Planck Institut für Plasmaphysik, Garching, W Germany.

Abstract

The resistive ballooning mode is studied in a separatrix geometry for parameters consistent with the H-mode. Besides the 'usual' ideal and resistive ballooning modes accessing a second stable regime at large plasma pressure gradients (α), we find another class of resistive ballooning modes, which do not stabilise as α increases. The properties of these modes are discussed in detail. Large pressure gradients associated with the H-mode, near the separatrix, can destabilise this class of rapidly growing resistive ballooning modes. We find that since these modes are stabilised by increasing plasma pressure, the possibility of a second stable window also exists for these resistive ballooning modes.

1 INTRODUCTION

The successive destabilisation and restabilisation of the ideal ballooning mode as the plasma pressure gradient is increased, has been known for some time [1]. The regime of stability at high pressure being termed the second stability regime. Access to the second stability regime can be improved by appropriate shaping of the flux surfaces. This has been achieved variously by indenting the plasma to form a bean shape [2] or by forming a magnetic separatrix on the small major radius side [3]. In fact for sufficiently indented 'beans', or sufficiently close to the separatrix, direct access to the second stable regime is possible, with no intervening period of instability as the pressure is raised. In the case of the separatrix geometry this direct access to second stability has formed the basis of a hypothesis [4] for explaining the L to H mode transition observed in many divertor tokamaks.

By considering the effect of resistivity the domain of ballooning instability is extended, relative to that for the ideal ballooning mode [5]. This is similar to the situation for low toroidal mode number (n) modes, where the inclusion of resistivity weakens the field line bending term and permits flux surface topology changes, which are destabilising [6]. Analytic formulations of the resistive ballooning problem have been made by several authors [7,8,9]. These analytic formulations are usually based on an outer resistive solution of the resistive ballooning equations which is matched asymptotically to the quantity Δ' determined by solving the ideal ballooning equations. As in tearing mode theory Δ' is the ratio of large to small Newcomb Solutions [10], and is a measure of the free energy available to drive the mode. For the resistive MHD model the criterion for ballooning instability is $\Delta' > \Delta'_c(> 0)$ [11]. Several authors have studied resistive ballooning stability by calculating Δ' values analytically [8,9]. Without recourse to the approximations necessary for analytic treatments Sykes et al have studied Δ' values numerically for a circular flux surface model equilibrium [12]. They found that the two fluid resistive stability boundary (Δ'=0) is in general very close to the ideal second stability boundary, although there are exceptions [13]. It should be noted, however, that inherent in the asymptotic matching procedure for the Δ'-formulation of the resistive ballooning problem is an assumption that the growth rate of the mode (γ) is much less than the sound frequency (γ_s). This is generally a good approximation. However, under certain conditions, such as those which occured in high-β_p, low temperature ISX-B shots [14], $\gamma > \gamma_s$ can occur. When $\gamma > \gamma_s$, then a new class of modes exists [15], whose growth rate is not related to Δ'; we shall call these electrostatic ballooning modes. An alternate regime in which one finds $\gamma > \gamma_s$, is near the separatrix in H-mode discharges - where the large local pressure gradients can cause large growth rates, but the relatively low

pressure causes γ_s to be small. Hahm and Diamond have analytically studied the properties of the electrostatic resistive ballooning mode for a double null separatrix geometry [16]. Linearly they find that the growth of electrostatic resistive ballooning modes is only weakly affected by the separatrix geometry. Nonlinearly however the large shear near the separatrix has been shown by Hahm and Diamond to greatly reduce the turbulent thermal conductivity due to the electrostatic resistive ballooning modes - this mechanism has been advanced as alternative explanation of the H-mode transition to that proposed by Bishop [4].

In this paper we will extend some of the resistive ballooning studies described above by solving the full resistive MHD ballooning equations. We are particularly interested in the properties of resistive modes in separatrix geometries. To elucidate the physics we use the simple separatrix equilibrium model described by Bishop [17]. Brief details of this and the resistive ballooning equations are given in Section 2. We start by studying the resistive stability in the second ideal stable regime for circular flux surface equilibria; these results are described in Section 3. Then, in Section 4, we extend this study to strongly shaped surfaces near a separatrix. We shall show that both classes of resistive ballooning modes predicted analytically (Δ' and electrostatic) occur and have important consequences for resistive stability in the second stable regime. These results are summarised and discussed in Section 5.

2 MODEL EQUATIONS

To study the generic features of resistive ballooning stability in separatrix geometry we use an analytic equilibrium solution. This exploits the fact that the equilibrium quantities required in the ballooning equations are local to a given flux surface and uses an expansion solution of the Grad-Shafranov equation in the vicinity of that flux surface. As this equilibrium model is explained in detail in Ref [17] we give only brief details here.

The equilibrium is determined once the flux surface shape and poloidal magnetic field on that surface are specified. The chosen flux surface shape in polar coordinates (r, θ) is specified as

$$k^2 = r^2(\sqrt{1+k}-1)^2(4 + r^2[\sqrt{1+k}-1]^2 - 4r\cos(\theta-\delta)[\sqrt{1+k}-1]), \qquad (1)$$

where δ is the location of the separatrix and k determines how distorted the flux surface is; k=0 is a circle and k=1 is the separatrix. Here r is normalised to its value r_0 opposite the separatrix ($\theta = \delta + 180°$). The corresponding poloidal field on the flux surface is specified by

$$b^2(\theta) = (1 + r^2[\sqrt{1+k}-1]^2 - 2r[\sqrt{1+k}-1]\cos[\theta-\delta])/(1+k), \qquad (2)$$

where again b is normalised to its value B_{p_0} at $\theta = \delta + 180°$. The various equilibrium terms such as curvature occuring in the ballooning equations can be calculated explicitly for this geometry by an inverse aspect ratio expansion. Using the form of the resistive ballooning equations given in Refs [5,9] the resulting equations for this equilibrium model are

$$\frac{b}{h}\frac{d}{d\theta}\left[\frac{b}{hL}\left\{\frac{1}{b^2}+P^2\right\}\frac{dU}{d\theta}\right] - \alpha K(U+V) - \gamma^2\left[\frac{1}{b^2}+P^2\right]U = 0 \qquad (3)$$

and

$$\frac{b}{hq_c^2}\frac{d}{d\theta}\left[\frac{b}{h}\frac{dV}{d\theta}\right] + \alpha K\left(\frac{4\gamma^2}{\alpha^2} + \frac{n^2}{S\gamma}\right)U$$
$$-\left\{\frac{n^2}{S\gamma}\left(-\alpha K + \gamma^2\left[\frac{1}{b^2} + P^2\right]\right) + \frac{\gamma^2}{q_c^2}\frac{1+\gamma_s^2}{\gamma_s^2}\right\}V \;=\; 0. \tag{4}$$

Here the growth rate γ is normalised to the Alfvén frequency $\gamma_A = B_{p_0}/(r_0\sqrt{\rho})$ with ρ the mass density; γ_s is the normalised sound frequency, $\gamma_s^2 = \Gamma P_0/B_0^2$ with B_0 and P_0 the magnetic field and pressure on the flux surface, respectively; q_c is the cylindrical safety factor; S the magnetic Reynolds number, is the ratio of the resistive to Alfvén transit time ($S = \tau_R/\tau_A$) with $\tau_R = r_0^2/\eta_0, \eta_0$ being the resistivity on the flux surface. The curvature term 'αK' is defined by

$$\alpha = \frac{-2r_0^2 P_0'}{B_{p_0}} \tag{5}$$

and

$$K = \frac{-1}{h}\left[P\left(\frac{dr}{d\theta}\cos\theta - r\sin\theta\right) + \frac{1}{b}\left(\frac{dr}{d\theta}\sin\theta + r\cos\theta\right)\right] \tag{6}$$

with

$$P = -b\int_{\theta_0}^{\theta}\frac{h}{b^3}\left[\frac{\alpha W}{D} - \Lambda + \frac{2b}{f} - \alpha r\cos\theta\right]d\theta \tag{7}$$

where the poloidal arc length is $hd\theta$ with $h = \sqrt{r^2 + (dr/d\theta)^2}$. The remaining quantities in Eq(7), W, D and the edge current density parameter Λ are defined in Ref [3]. To complete these definitions

$$L = 1 + \frac{n^2 q_c^2}{S\gamma}\left[\frac{1}{b^2} + P^2\right]. \tag{8}$$

The appearance of the parameter θ_0 in Eq (7) should be noted. This is a free parameter ($0 \le \theta_0 < 2\pi$) over which the growth rate (γ) must be maximised. In the circular flux surface limit ($k = 0$) $D = b = h = 1, W = 0$,

$$P = \hat{S}(\theta_0 - \theta) + \alpha(\sin\theta - \sin\theta_0) \tag{9}$$

and

$$K = P\sin\theta - \cos\theta, \tag{10}$$

with $\hat{S} = r_0 q'/q$ being the shear. In this limit ($k = 0$) we recover the 'normal' $\hat{S} - \alpha$ ballooning equations [18]. The ballooning equations (3) and (4) are either solved using a standard eigenvalue package [19] or using the variational approach described in Ref [5]; the results of both methods being in excellent agreement.

Finally we note that although this equilibrium is very simple it does appear to retain the salient features of separatrix equilibria – in the ideal limit, solutions of the ballooning equations for numerical equilibria, on flux surfaces near a separatrix, produce qualitatively very similar results to those obtained with this model separatrix equilibrium (Eqs (1) and (2)) [20].

3 CIRCULAR FLUX SURFACE LIMIT

In the $\hat{S} - \alpha$ limit, Sykes et al [12] have studied resistive ballooning mode stability by evaluating Δ' values. These are related to the growth rate within the context of resistive MHD theory by [7,8]

$$\Delta' = \frac{2\gamma^{5/4}(1+2q_c^2)^{1/4}}{\left(n^2\hat{S}^2q_c^2/S\right)^{3/4}}\left[\frac{\Gamma(1/4)}{\Gamma(3/4)} - \frac{\Gamma(1/4+\hat{\gamma}^{3/2}/4)}{\Gamma(3/4+\hat{\gamma}^{3/2}/4)}\right]^{-1} \tag{11}$$

where $\hat{\gamma} = \gamma/\gamma_R$ and $\gamma_R^3 = n^2\hat{S}^2q_c^2\gamma_s^4(1+2q_c^2)/S$. Figure 1 shows a comparison of this dispersion relation with the code results in the first stability zone for $\hat{S} = 1, n^2/S = 5 \times 10^{-5}, q_c = 3, \theta_0 = 0$, and $\gamma_s^2 = 2.5 \times 10^{-3}$. For $\alpha < 0.5$ the dispersion relation and code results agree quite well but as the ideal threshold is approached ($\alpha = 0.61$) the assumptions made in deriving the dispersion relation break down and the agreement worsens.

For the $\hat{S} - \alpha$ model Sykes et al [12] have also calculated Δ' values in the second stable region. They find the $\Delta' = 0$ boundary lies very close to the ideal boundary and thus resistive ballooning modes are largely stable in the second stable regime. Under certain circumstances, however, we find a class of ballooning instabilities, not accounted for in the Δ' treatment, can be unstable in the second (ideal) stable regime. Figure 2 shows the real part of the growth rate as a function of α for $\gamma_s^2 = 3 \times 10^{-3}, q_c = 3, n^2/S = 5 \times 10^{-5}, \hat{S} = 1$ and $\theta_0 = 0$. (Here we use the representation $e^{\gamma t}$ and so the imaginary part of γ corresponds to a frequency and the real part to a growth rate). Two distinct branches can be seen in Fig 2; the 'inverted U curve' closely parallels the ideal marginal stability curve and corresponds to the modes represented by the Δ' theory. The other branch corresponds to a class of electrostatic modes. The Δ'-branch has a second stable regime, i.e. the growth rate vanishes for all α values above a critical one. In contrast the electrostatic modes do not stabilize when α is increased (but are stabilised at small α-values). Consequently for these values of β, n^2/S and safety factor q_c, the electrostatic modes are unstable when the Δ'-mode is in the second stable regime. The electrostatic branch in Fig 2 has a bifurcation for $\alpha \sim 2.2$. This occurs when the two purely growing solutions for $\alpha > 2.2$ coalesce and the solutions become overstable (for $\alpha < 2.2$). The Δ'-branch also has overstable behaviour for small γ [7,11], but for the parameter values used in Fig 2 these overstable solutions lie very close to the real branch and are not shown. In this first stable regime the overstable roots are damped for $\Delta' < \Delta'_c(\propto \beta^{5/6})$ [11] and so the region of instability increases as β decreases.

In the fully compressible limit ($\Gamma \to 0$) the plasma is ballooning unstable, to electrostatic modes, for all values of α [21]. The electrostatic resistive ballooning modes are discussed in Refs [15], and they occur in the regime $\gamma > \gamma_s$ (the opposite to that assumed in deriving the Δ' branch). We repeat brief details of a derivation of a dispersion relation for these modes to elucidate their properties. In the limit $\gamma_s = 0$ the resistive ballooning equations become

$$\frac{S\gamma}{n^2q_c^2}\frac{d^2U}{d\theta^2} - \alpha(P\sin\theta - \cos\theta)U - \gamma^2(1+P^2)U = 0, \tag{12}$$

where P is defined by Eq(9) and we have made an electrostatic approximation

$$\gamma \ll \frac{n^2P^2q_c^2}{S}. \tag{13}$$

Note that this approximation corresponds to relatively extended modes (in θ). To solve Eq(12) we assume eigenfunctions (of U) of the form of an envelope function $\bar{U}$ and a superimposed oscillation of scale length 2π, $\tilde{U}$. Thus $U = \bar{U} + \tilde{U}$ and we assume $\bar{U} \gg \tilde{U}$. Equating fluctuating and average terms in Eq(12) we obtain with $P \gg 1$

$$\frac{S\gamma}{n^2 q_c^2}\frac{d^2\bar{U}}{d\theta^2} + P^2\left(\frac{n^2 q_c^2 \alpha^2}{2S\gamma} - \gamma^2\right)\bar{U} = 0. \tag{14}$$

This is a Weber equation for which the fastest growing eigenvalue satisfies

$$\gamma^3 = \frac{n^2 q_c^2 \alpha^2}{2S}. \tag{15}$$

This result is derived in Refs [7,15] and gives the growth rate of the electrostatic modes in the pressure convection limit ($\gamma_s = 0$). By solving perturbatively in γ_s we can obtain a correction to Eq(15)

$$\gamma^3 + \gamma_s^2\gamma(1 + 2q_c^2) = \frac{n^2\alpha^2 q_c^2}{2S}. \tag{16}$$

The solution of this dispersion relation (broken line) is compared with the numerical result (solid line) in Fig 2. For this case $\gamma_s = 5.5 \times 10^{-2}$. It can be seen from Fig 2 that the dispersion relation and numerical results are in good agreement when $\gamma > \gamma_s$.

From Eq(16) we see that increasing the sound frequency (γ_s) has a stabilising effect. This is confirmed in Fig 3 which is identical to Fig 2 except that $\gamma_s^2 = 10^{-2}$. Comparing Figs 2 and 3 it can be seen that the Δ'-branch ('inverted U') is relatively unaffected by raising the sound frequency but the electrostatic modes are strongly stabilised. At $\gamma_s^2 = 10^{-2}$ there is now a 'window' of second resistive ballooning mode stability in which the Δ' and electrostatic modes are stable.

Until now we have presented results with $\theta_0 = 0$. For the Δ' modes we find the region of resistive ballooning instability in the second regime is maximised by this choice, in agreement with Ref [12]. For the electrostatic ballooning modes we find their growth rate to be essentially independent of θ_0 — a result expected from the analytic theory. This is shown in Fig 4 where the growth rate versus θ_0 is plotted for $\alpha = 3, n^2/S = 5\times10^{-5}, \gamma_s^2 = 2.5\times10^{-3}, \hat{S} = 0.5$, and $q_c = 3$. Also from the analytic theory we expect the growth rate of the electrostatic modes to be independent of shear ($\hat{S}$). This is again confirmed by the computational solutions; results are shown in Fig 5 for the parameters $\alpha = 3, \theta_0 = 0, n^2/S = 5 \times 10^{-5}, \gamma_s^2 = 2.5 \times 10^{-3}$ and $q_c = 3$.

4 SEPARATRIX RESULTS

We find the same basic behaviour for finite k as we do in the $\hat{S} - \alpha$ ($k = 0$) limit. Figure 6 shows the growth rate of the resistive ballooning modes as a function of α for $\Lambda = 0.8, k = 0.82, \theta_0 = -1.0, \delta = 3\pi/4, q_c = 2.5$, and $\gamma_s^2 = 2.5 \times 10^{-3}$. The qualitative similarity between the $\hat{S} - \alpha$ results shown in Fig 2 and the $k = 0.82$ results in Fig 6 is evident. Again for the Δ'-branch ('inverted U') overstable roots (broken curves) occur at the smaller growth rates. This behaviour is predicted by the general form of the dispersion relation Eq(11) as discussed in Ref [7]. For the electrostatic modes we see that instability persists in the second ideal stable regime. The dispersion relation (Eq(16)) derived for the electrostatic modes is

only applicable in the $\hat{S} - \alpha$ limit. We may however generalise the analysis, as was done in Ref [16] for a double null separatrix equilibrium, to $k \neq 0$. In this case we make an expansion in inverse powers P/b [7]. The result is

$$\gamma^3 + \gamma\gamma_s^2 \left(2q_c^2 + \frac{1}{\Delta}\right) = \gamma_c^3 \Delta \tag{17}$$

with

$$\gamma_c^3 = \frac{n^2\alpha^2 q_c^2}{2S} \tag{18}$$

$$\Delta = \frac{\left[\langle hg^2/b\rangle \langle h/b\rangle - \langle 2hg\cos\theta/b\rangle^2\right]}{\langle hb\rangle \langle h/b\rangle} \tag{19}$$

and

$$\langle x\rangle = \frac{1}{2\pi}\int_0^{2\pi} x d\theta. \tag{20}$$

Evaluating Eq(19) in the $\hat{S} - \alpha$ limit we find $\Delta = 1$, and so Eq(17) is consistent with Eq(16). The parameter Δ (and thus the growth rate γ) increases monotonically with k. Figure 7 shows a comparison of this dispersion relation with numerical results for the same parameters as Fig 6. As in the $S - \alpha$ limit we see from Eq(17) that the electrostatic modes should have a weak θ_0 dependence. We find this to be so numerically and will not discuss the θ_0-dependence further in this section.

Also we see from Eq(17) that increasing the sound frequency has a stabilising influence on the electrostatic modes. This is confirmed in Fig 8 which is identical to Fig 6 except that the sound frequency has been increased to $\gamma_s^2 = 5 \times 10^{-3}$.

A convenient way of representing these results is to plot growth rate contours in the $\alpha - k$ plane. Figure 9 shows such a plot for $n^2/S = 5 \times 10^{-5}, \gamma_s^2 = 2.5 \times 10^{-3}, q_c = 2.5$, $\theta_0 = -1$, and $\delta = 3\pi/4$. The $\gamma = 2 \times 10^{-2}$ contour (which passes through $k = 0.5, \alpha \sim 0.4$), closely parallels the ideal marginal contour and is related to the Δ'-branch. While the remaining γ-contours, which remain unstable into the second regime are electrostatic resistive ballooning modes. For large k the contours turn-up sharply. This behaviour is not reproduced by the dispersion relation since in this region of parameter space the assumption of slow variation of P/b over one field period is no longer valid. The gaps in the curves of Fig 9 are related to the Δ' and electrostatic branches becoming degenerate at the points where they cross. In the $\alpha - k$ plane this degeneracy manifests itself through the joining of the Δ' and electrostatic branches. We have not examined the continuity of the branches in this degenerate region in detail and hence leave the small gaps. Note that the electrostatic mode with $\gamma = 5 \times 10^{-3}$ becomes overstable for $k < 0.9$ and we have therefore omitted that part of the solution from Fig 9. It can be seen from Fig 9 that the electrostatic modes remain unstable in the region of $k \sim 1.0$ where complete stability to the ideal modes occurs. This suggests that transport from the electrostatic ballooning modes may play a role in the H-mode [16].

An important feature of the ideal ballooning modes is that the point where the first and second regimes coalesce moves to smaller k values as the current density near the separatrix (Λ) increases. This feature forms an important component of the L to H transition model proposed by Bishop [4]. From Eq (17) however, it is evident that we do not expect a strong dependence on Λ for the electrostatic modes. This is confirmed in Fig 10 which shows the variation of the growth rate with Λ for Δ'-modes (solid line) and electrostatic modes (dashed

line) with $\alpha = 1, k = 0.82$ and all other parameters as in Fig 9. The electrostatic modes are basically unaffected by varying Λ and in fact near $k = 1.0$ they are slightly destabilised at larger Λ. This lack of dependence of the growth rate on Λ is the analogue of the shear independence in the $\hat{S} - \alpha$ limit (Fig 5).

As discussed in the introduction it is the relatively high pressure gradients and low pressure (and therefore γ_s) values near the spearatrix in the H-mode which favours the growth of the electrostatic modes. By raising the β-values near the separatrix we can stabilise the electrostatic ballooning modes. This is shown in Fig 11 for $k = 0.95, n^2/S = 5 \times 10^{-5}, \Lambda = 0.8, q_c = 2.5$, $\delta = 3\pi/4$ and $\alpha = 0.8$. The change in gradient of the curve for $\beta \sim 0.4$ is associated with the mode becoming overstable. The stabilising effect of increasing β is evident in Fig 11 but for realistic H-mode parameters it is not expected that this effect will stabilise the electrostatic modes in the vicinity of the separatrix (see Section 5). In principle, however, electrostatic modes can be stabilized by large β, whereas Δ'-modes remain relatively unaffected. This provides us with the possibility, as in the circular case ($k = 0$), of achieving a second stable window in the region where the Δ'-mode is already stabilized and the electrostatic mode is not yet unstable.

We finally turn to the dependence of the ballooning instability on δ, the poloidal location of the separatrix. From the dispersion relation (Eq 17) we expect the growth rate to increase monotonically with decreasing δ. We have found this to be the case for small k (< 0.6), but at large k (where the dispersion relation is invalid) we find that varying δ can have a significant effect. Figure 12 shows γ-contours in the $\alpha - k$ plane for $\delta = 2$ and π, with $\Lambda = 0.8$, $n^2/S = 5 \times 10^{-5}, \gamma_s^2 = 2.5 \times 10^{-3}$, and $\theta_0 = -1$. For $\delta = 2$ and $k \sim 0.9$ there are many nearby branches, which makes the tracking of a given root difficult; those shown are the most unstable roots found (ie smallest α for a given growth rate). Comparing Figs 9 and 12 it can be seen that the electrostatic modes are strongly stabilised for $\delta = \pi$, relative to the $\delta = 3\pi/4$ case. In particular the electrostatic modes do not remain strongly unstable in the coalesence region at high k when $\delta \sim \pi$. This behaviour is not reproduced by the dispersion relation (Eq(17)) because the variation in P over a field period becomes large compared with P itself. Defining $\tilde{P} = P - \langle P \rangle$ we can treat $\tilde{P}$ as a pertubative correction to the $\gamma_s = 0$ dispersion relation. The result is

$$\gamma^3 + \lambda\gamma^2 = \gamma_c^3 \Delta \tag{21}$$

where

$$\lambda = -\frac{2n^2q^2\alpha}{\langle bh \rangle S} \left\langle \left(\frac{h}{b} \int_0^\theta \tilde{P} h b d\theta \right) \left(\frac{\langle hg \cos\theta/b \rangle}{\langle h/b \rangle} - g\cos\theta \right) \right\rangle \tag{22}$$

Evaluating λ we find it is positive and increases monotonically with k and δ ($\pi/2 < \delta < \pi$). Equation (21) thus qualitatively reproduces the strong δ–dependence, but since it does not contain the sound wave corrections ($\gamma_s \neq 0$) we can not compare quantitatively.

5 CONCLUSIONS AND DISCUSSION

The properties of the resistive ballooning modes have been studied for a class of separatrix equilibria. Two distinct branches of the resistive ballooning mode have been identified. Analytically these branches are distinguished by the assumed ordering between the growth rate (γ) and sound frequency (γ_s). If $\gamma_s \gg \gamma$ is assumed then ballooning modes driven by free

energy (Δ') from the ideal region occur. In the alternate limit ($\gamma \gg \gamma_s$) electrostatic resistive ballooning modes occur. Numerically in the regime $\gamma \sim \gamma_s$ we find that both branches can co-exist. At small values of γ the Δ'-mode develops additional overstable branches at the low, as well as on the high, α side. Similarly the electrostatic modes become overstable at small values of α, where its slow and fast growing branches join. In contrast to the Δ'-modes, the electrostatic modes are not stabilized if α is increased. The only possibility for a second stable regime to exist is therefore at large values of β, where the threshold for instability of the electrostatic mode is shifted to large values of α and a stable 'window' between Δ' and electrostatic modes exists. Since most proposals for achieving the second ideal stable regime in non-separatrix tokamaks [22,23] involve high β (as well as high α) we expect this window should exist in these cases. Using the values given in Ref [22] for example we find that the expected β should be sufficient to provide a second resistive ballooning stable window.

Near the separatrix in the H-mode the high pressure gradients and relatively low pressure lead to the regime $\gamma \gtrsim \gamma_s$ and thus the electrostatic modes are important. Using published values of temperature and density gradients for D-III-D [24] for example we find that the region $\gamma > \gamma_s$ should extend over the separatrix region, for $n \gtrsim 10$. For the Δ'-driven and ideal modes the regions of instability (and growth rates) are sensistive to the edge current density (Λ). For the electrostatic modes however there is a weak dependence on Λ. The electrostatic modes are however sensitive to the separatrix location (δ). The region of instability to the electrostatic modes is maximised by the choice $\delta \sim 2.4$ (when the parameters are as for Fig 9) and is considerably reduced for $\delta \sim \pi$.

In the cases where the electrostatic modes remain unstable in the coalesence region it is important to study their effects on energy and particle transport. This has been done by Hahm and Diamond [16] who show that high shear near the separatrix leads to greatly reduced transport (despite the weak effect of the separatrix on the linear growth rate). Finally we remark that the strong density gradients near the separatrix in the H-mode mean that diamagnetic effects ($\omega_\star$) should be important. These effects will be discussed in a future publication.

Acknowledgements

We thank C.Bishop and J.Hastie for their help during the course of this work.

References

[1] Coppi,B., Ferreira,A., Ramos,J.J., Phys.Rev.Lett. **44** (1980) 990.
Mercier,C., Plasma Physics and Controlled Fusion Research (IAEA, Vienna), Vol. I (1979) 701.
Lortz,D., Nührenberg,J., Phys.Lett. **68a** (1978) 49.
Strauss,H.R., Park,W., Monticello,D.A., et al, Nucl.Fus. **20** (1980) 638.
Greene,J.M., Chance,M.S., Nucl.Fus. **21** (1981) 453.

[2] Todd,A.M.M., et al., Nucl.Fus. **19** (1979) 743.

[3] Bishop,C.M., Nucl.Fus. **26** (1986) 1063.

[4] Bishop,C.M., Nucl.Fus. **27** (1987) 1765.

[5] Zehrfeld,H.P., Grassie,K., Nucl.Fus. **28** (1988) 891.

[6] Furth,H.P., Killeen,J., Rosenbluth,M.N., Phys.Fluids **6** (1966) 101.

[7] Connor,J.W., Hastie,R.J., Martin,T.J., Sykes,A., Turner,M.F., Plasma Physics and Controlled Nuclear Fusion Research (IAEA, Baltimore), Vol. III (1983),403.

[8] Drake,J.F., Antonsen,T.M., Phys Fluids **28** (1985) 544.

[9] Correa-Restrepo,D., Z.Naturforsch. **37a** (1982) 848.

[10] Newcomb,W.A., Annals Phys **10** (1960) 232.

[11] Chance,M.S., et al., Plasma Physics and Controlled Nuclear Fusion Research (IAEA, Vienna), Vol. I (1979) 677.

[12] Sykes,A., Bishop,C.M., Hastie,R.J., Plasma Physics and Controlled Nuclear Fusion **29** (1987) 719.

[13] Correa-Restrepo,D., Plasma Physics and Controlled Fusion **27** (1985) 565.

[14] Carreras,B.A., Diamond,P.H., Murakami,M., et al, Phys Rev Lett **50** (1983) 503.

[15] Hender,T.C., Carreras,B.A., Cooper,W.A., Holmes,J.A., Diamond,P.H., Similon,P.L., Phys.Fluids **27** (1984) 1439.

[16] Hahm,T.S., Diamond,P.H., Phys.Fluids **30** (1987) 133.

[17] Bishop,C.M., Culham Report CLM-R 249 (1985).

[18] Connor,J.W., Hastie,R.J., Taylor,J.B., Phys.Rev.Lett. **40** (1978) 396.

[19] Lord,M.E., Scott,M.R., Watts,H.A., applied Nonlinear Analysis (Academic, New York, 1979), 635-656.

[20] Roy,A., Troyon,F., Proceedings of the Int. School of Plasma Physics, Varenna 1987, 143.

[21] Kadomtsev,B.B., Pogutse,O.P., Yurchenko,E.I., Plasma Physics and Controlled Nuclear Fusion Research, IAEA Baltimore 1982, 67.

[22] Sabbagh,S.A., Hughes,M.H., Phillips,M.W., Todd,A.M.M., and Navratil,G.A., 'Transition to the Second Region of Ideal MHD Stability', Submitted To Nuclear Fusion.

[23] Yamazaki,K., Naitou,H., Amano,T., et al, in Plasma Physics and Contr Nuclear Fusion Research (Proc 11th Int Conf Kyoto 1986) Vol 2 IAEA Vienna, (1987) 27.

[24] Ohyabu,N., Burrell,K.H., Carlstrom,T.N., et al, Proc 15th European Conf on Contr Fusion and Plasma Heating (European Physical Society Dubrovnik 1988), Vol I, 227.

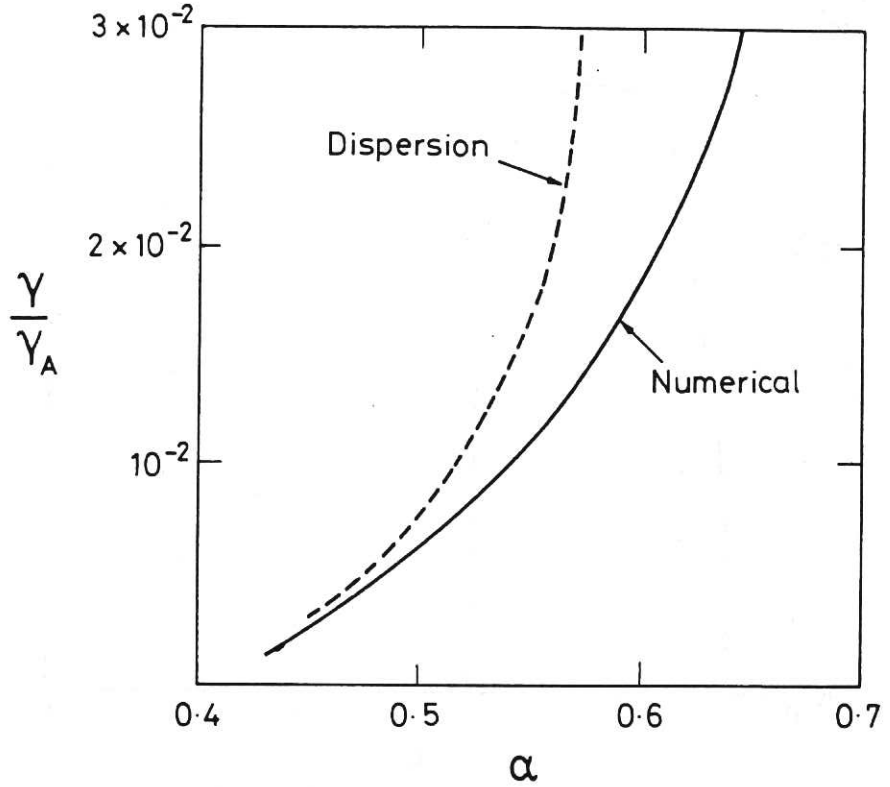

Fig. 1 Growth rate γ (normalised to γ_A) versus α for Δ'-modes in the first stability regime, numerical (solid line) and dispersion relation (dashed line) results are shown. The parameter values are $n^2/S=5\times10^{-5}$, $\gamma_s^2=2.5\times10^{-3}$, $\hat{S}=1,\theta_0=0$ and $q_c=3$.

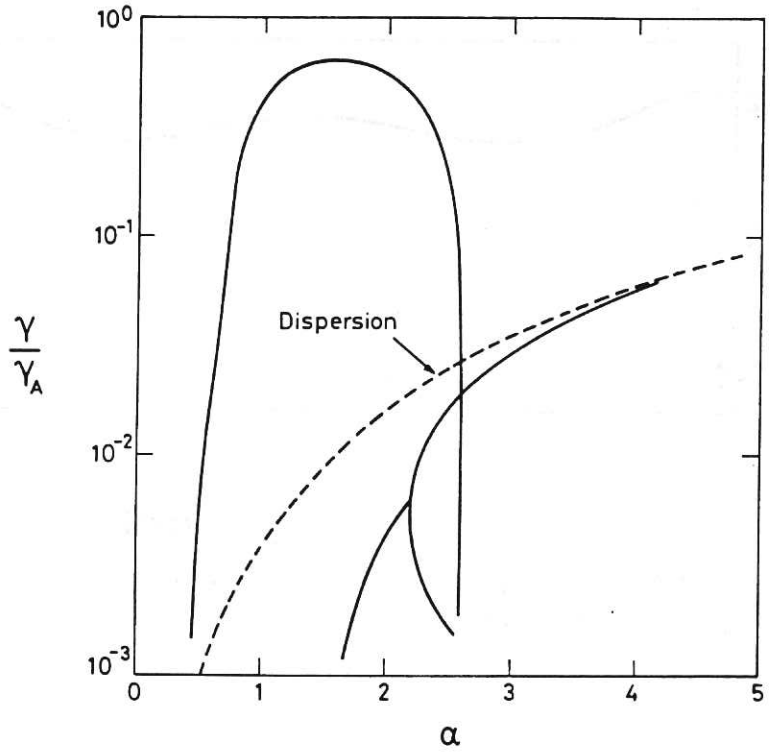

Fig. 2 Growth rate γ versus α. Results are shown for the Δ'-mode ('inverted U') and electrostatic mode. The parameter values are $n^2/S=5\times10^{-5}$, $\gamma_s^2=3\times10^{-3}$, $\hat{S}=1,\theta_0=0$ and $q_c=3$. Results from the dispersion relation for electrostatic modes Eq(16) are represented by the dashed curve.

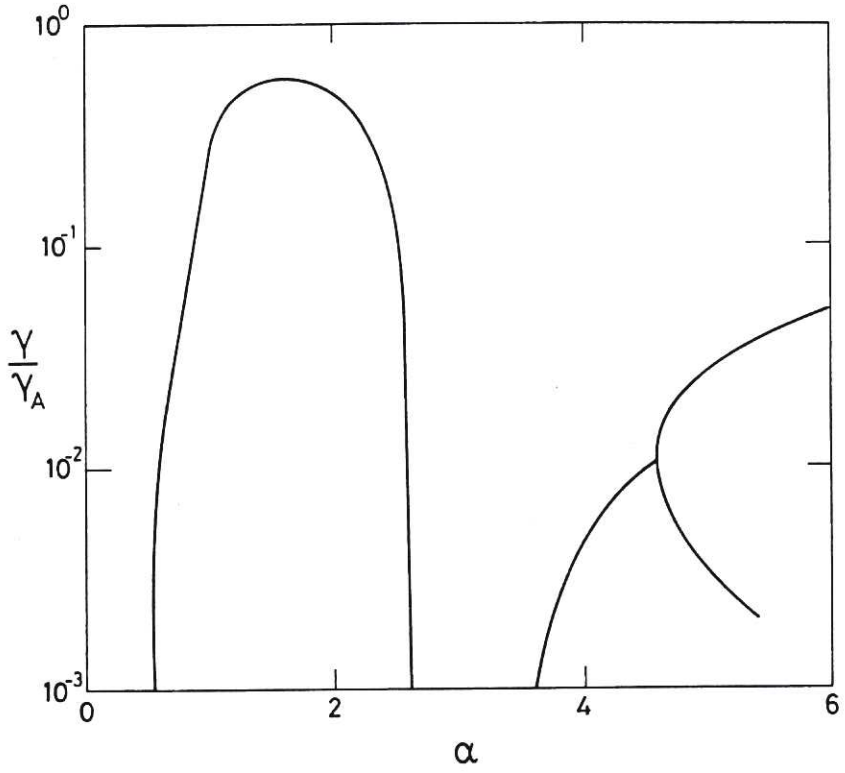

Fig. 3 As Fig. 2 but for larger sound frequency ($\gamma_s^2=10^{-2}$).

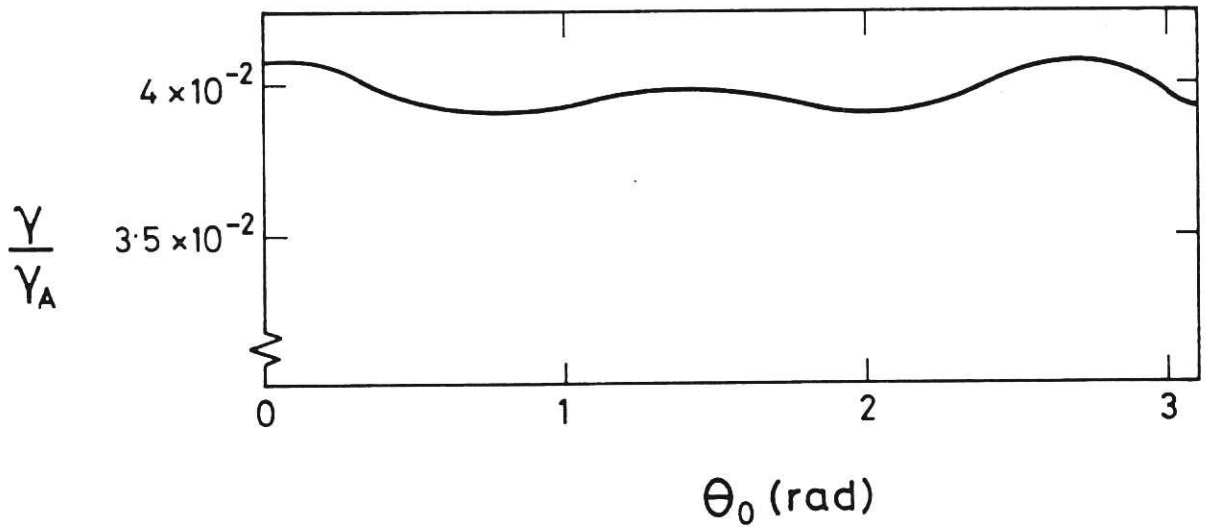

Fig. 4 Growth rate versus θ_0 for electrostatic ballooning modes. Parameter values are $\alpha=3$, $n^2/S=5\times10^{-5}$, $\gamma_s^2=2.5\times10^{-3}$, $\hat{S}=0.5$ and $q_c=3$.

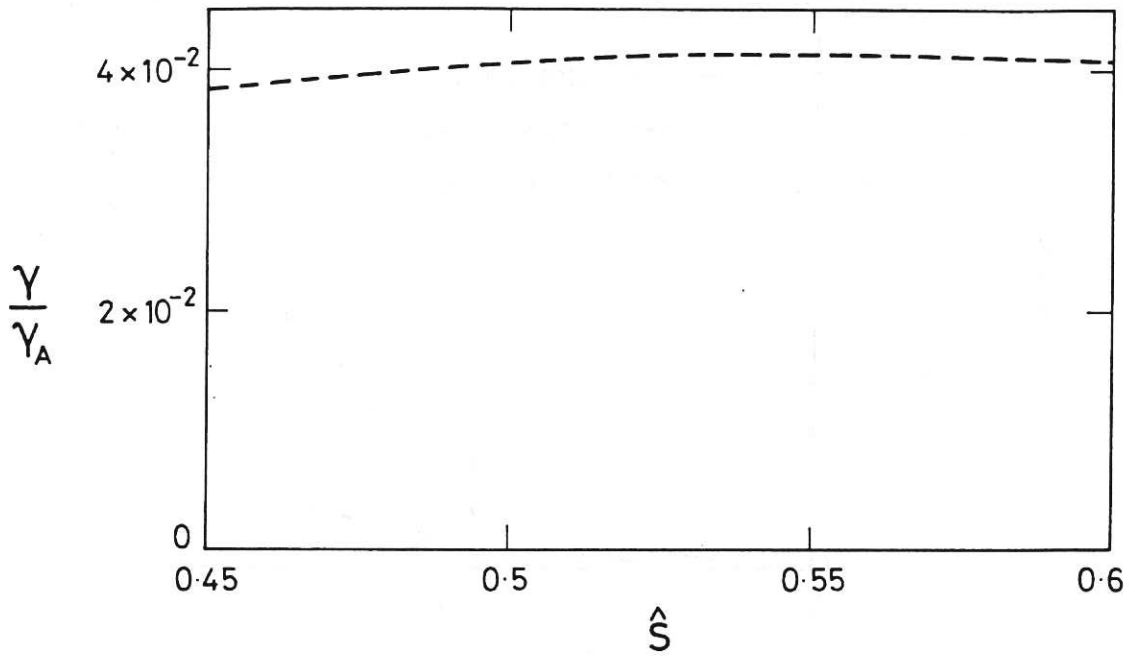

Fig. 5 Growth rate γ versus shear for electrostatic ballooning modes with $n^2/S=5\times10^{-5}$, $\gamma_s{}^2=2.5\times10^{-3}$, $\alpha=3$, $\theta_0=0$ and $q_c=3$.

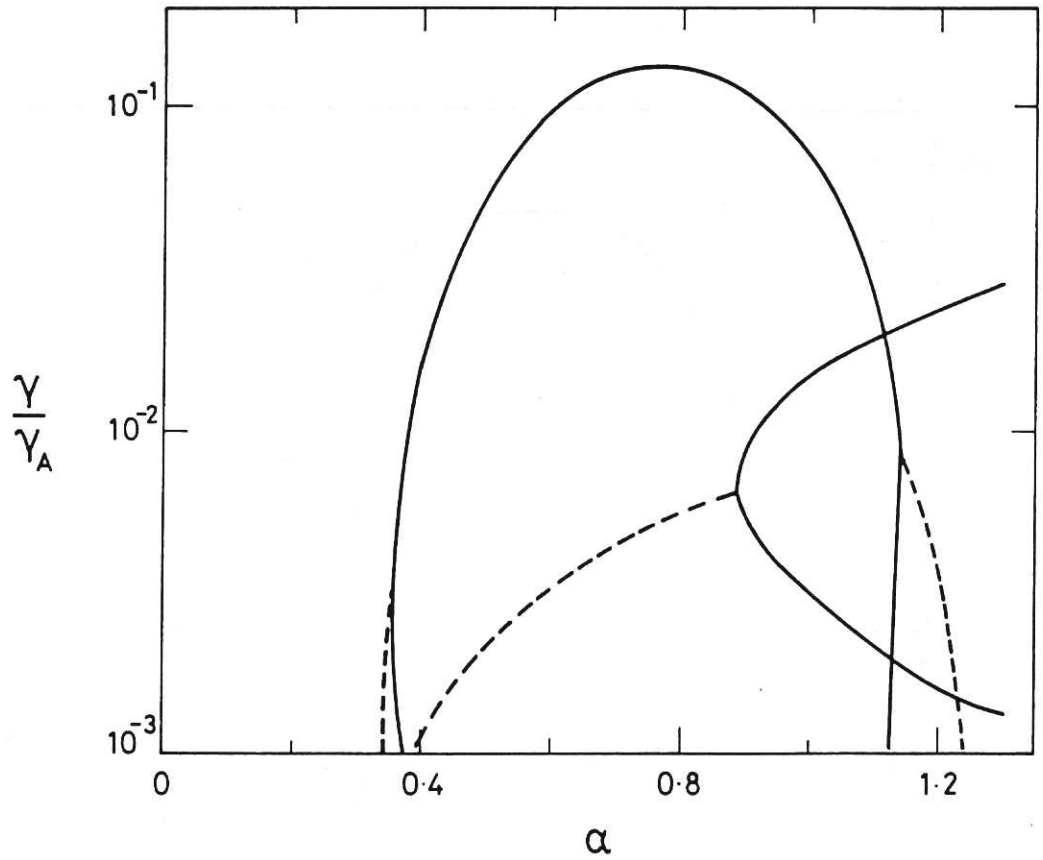

Fig. 6 Growth rate γ versus α for Δ' and electrostatic modes. The parameter values are $n^2/S=5\times10^{-5}$, $\gamma_s{}^2=2.5\times10^{-3}$, $\Lambda=0.8$, $\theta_0=-1$, $\delta=3\pi/4$, $k=0.82$ and $q_c=2.5$. The broken curves represent overstable growth.

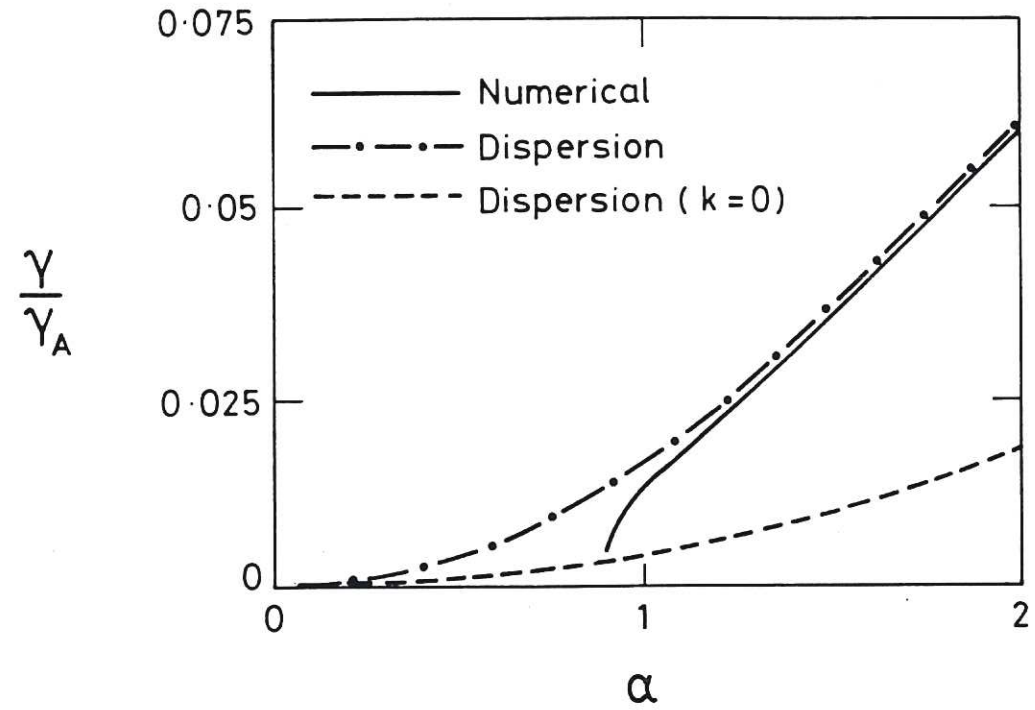

Fig. 7 Growth rate γ versus α for electrostatic modes. The parameter values are as in Fig. 6. For comparison we also give the result from the dispersion relation in the circular limit, $k=0$ (short dashed line).

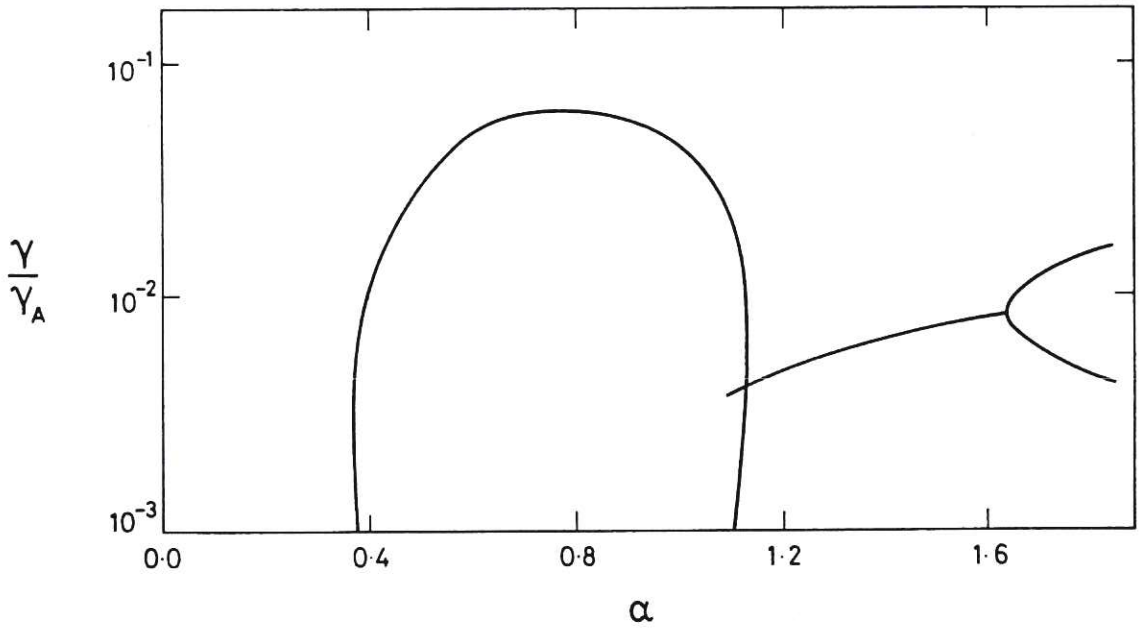

Fig. 8 Same as Fig. 6 but with increased sound frequency $\gamma_s^2=5\times10^{-3}$.

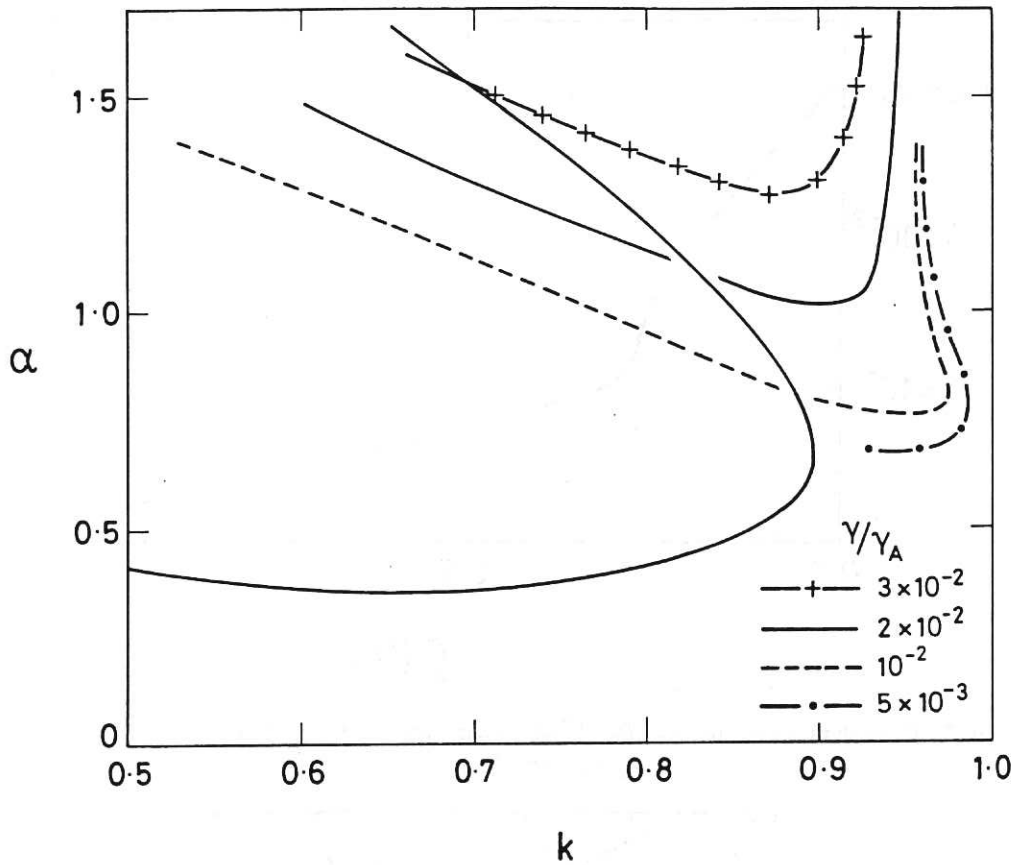

Fig. 9 Growth rate contours in the α versus k plane with $n^2/S=5\times10^{-5}$, $\theta_0=-1$, $q_c=2.5$, and $\gamma_s^2=2.5\times10^{-3}$.

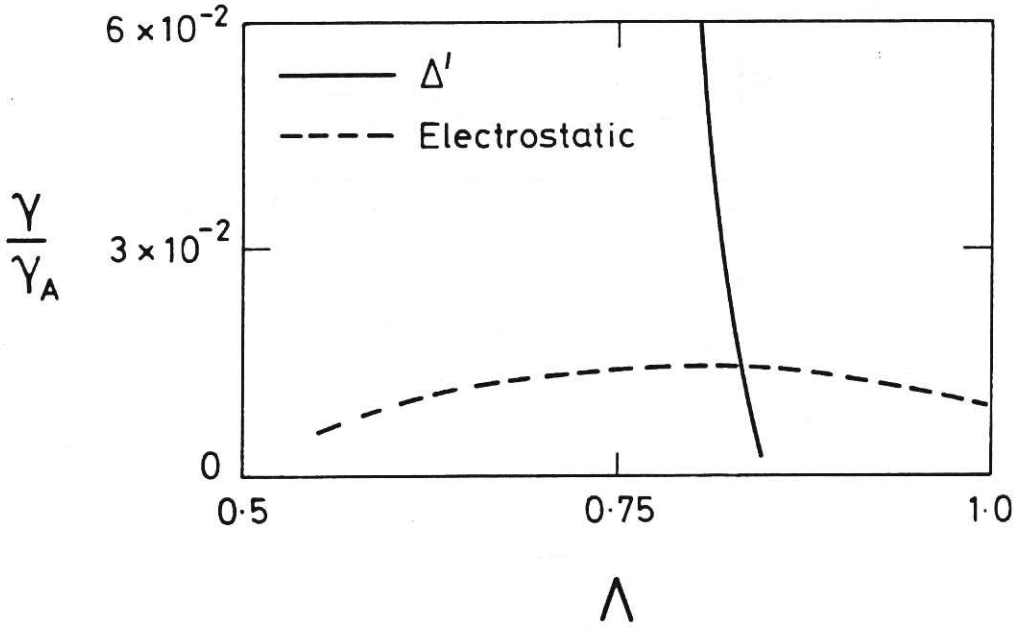

Fig. 10 Growth rate versus current density parameter Λ for Δ'-modes (solid line) and electrostatic modes (dashed line). The parameters are as in Fig. 9 with $k=0.82$ and $\alpha=1.0$.

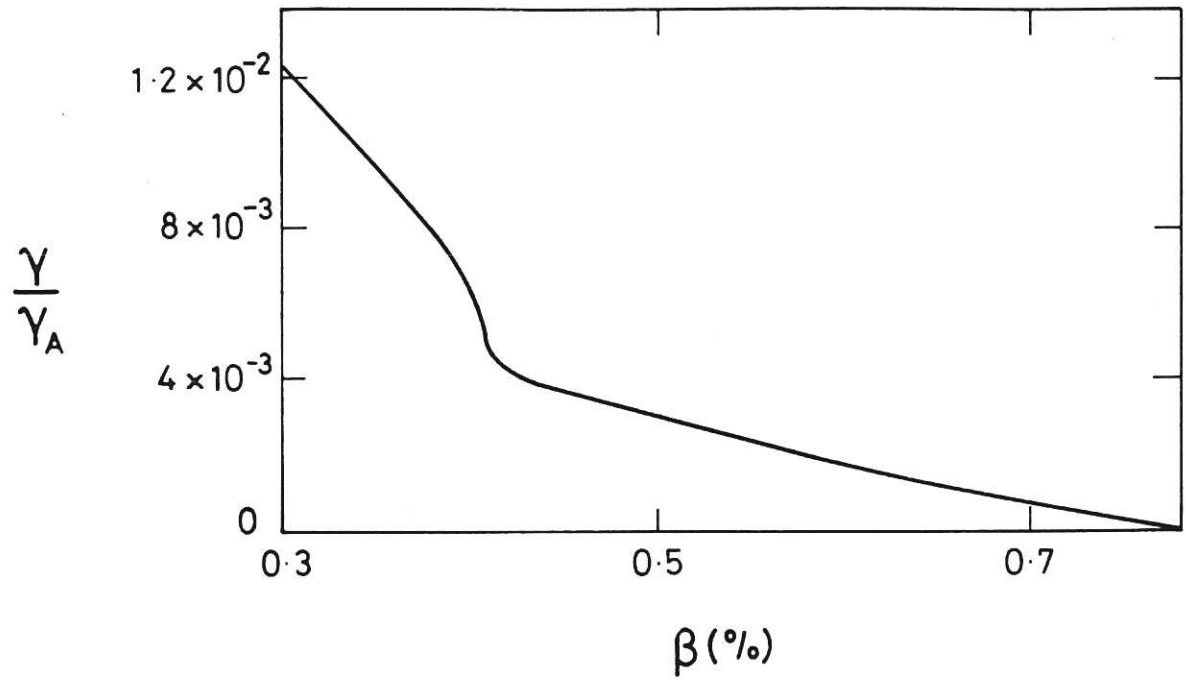

Fig. 11 Growth rate γ versus $\beta(=2P_0/B_0^2)$ for $\alpha=0.8$ with $k=0.95$, $n^2/S=5\times10^{-5}$, $\Lambda=0.8$, $q_c=2.5$ and $\delta=3\pi/4$.

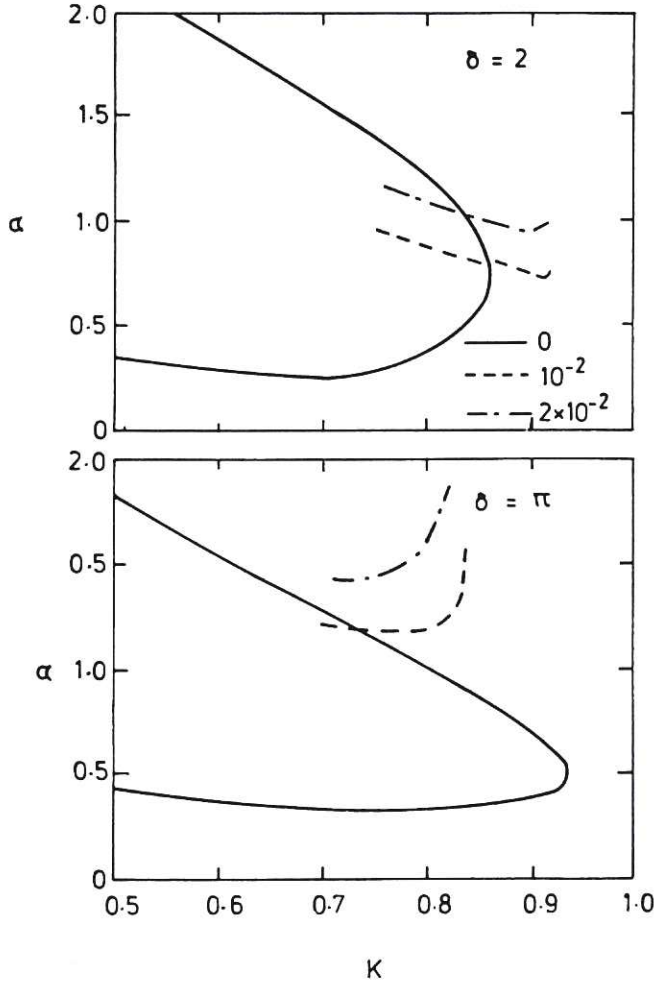

Fig. 12 Growth rate contours in the α-k plane for $\delta=2$ and π with $\theta_0=-1$, $n^2/S=5\times10^{-5}$, $\Lambda=0.8$, and $\gamma_s^2=2.5\times10^{-3}$.